HBRC Journal (2013) 9, 1–14

Housing and Building National Research Center

HBRC Journal

http://ees.elsevier.com/hbrcj

Developing an ANN model to simulate ASTM C1012-95 test considering different cement types and different pozzolanic additives

O.A. Hodhod [a], G. Salama [b,*]

[a] Struct. Eng. Dept., Faculty of Engineering, Cairo University, Egypt
[b] Civil Eng. Dept., Faculty of Engineering, Cairo University, Egypt

Received 6 February 2012; accepted 11 November 2012

KEYWORDS

Sulfate attack;
Cement type;
Fly ash;
GGBFS;
ASTM C1012 test method;
Artificial neural networks (ANN)

Abstract The primary factors affecting concrete sulfate resistance are the chemistry of Portland cement and the replacement level of mineral admixtures [1]. In order to investigate the effect of those on the sulfate attack the testing program in the literature involved the testing of different mortar mixes using the standardized test, ASTM C1012-95. ASTM C1012-95 has been widely used by researchers to study the sulfate resistance of cement based materials by exposing 1∗1∗11 in. mortar specimens to 50 g/L Na_2SO_4 or $MgSO_4$ solution [2]. However, there are deficiencies in this test method including lengthy measuring period, insensitivity of the measurement tool to the progression of sulfate attack, the effect of curing and the effect of the pH change during the time in the solution [3–5].

In this research a study is presented to build a model by ANN equivalent to ASTM C1012-95. The input parameter was obtained from 16 different mortars according to ASTM C1012-95. Plain Portland cement mortars, mortars with cement combined with fly ash (FA), and mortars with cement combined with slag (GGBFS) were tested by using ASTM C1012-95. Four cements, two ratio of FA, and one GGBFS were obtained from the literature. ASTM C1012-95 modeling techniques can help us understand the influence of aggressive environments on the concrete performance more readily, faster, and accurately. Such an understanding improves the decision making process in every stage of construction and maintenance and will help in better administration of resources.

* Corresponding author.

☆ Peer review under responsibility of Housing and Building National Research Center.

Production and hosting by Elsevier

Introduction

Many researchers have investigated the interaction between hydrated cement paste and sulfate compounds. The first approaches to characterizing sulfate attack were undertaken back in the 1920s by Thorvaldson, wherein the chemical interactions of individual pure states of Portland cement components in

1687-4048
http://dx.doi.org/10.1016/j.hbrcj.2013.02.003

water and solutions of alkali salts were studied. He proposed simple approaches and practical methods for carrying out these tests and formulated remedies as a direct result of his investigations. His research findings were acknowledged early on as the major turning point in research on the sulfate problem [6].

Thorvaldson recognized that a cure might be affected through a modification of the chemical composition of Portland cement. He also stipulated that calcium trisulfoaluminate, better known as ettringite, is a typical product of the reaction between hydrated C_3A and Na_2SO_4 solutions at all concentrations, and $MgSO_4$ solutions at low concentrations [6].

As early as 1890, Candlot had already associated the formation of ettringite crystals with concrete expansion. It was then known as the ''cement bacillus''.

Nearly 40 years later, Thorvaldson explored this phenomenon as the basis for developing the mortar bar expansion test in order to correlate the chemical and microstructure changes with the behavior of concrete exposed to sulfate solutions. The test procedure, later refined, is well known in the modern era for providing a quantitative evaluation of the contribution of Portland cement constituents in the presence of other substances to the expansion of paste or mortar bars. The findings from Thorvaldson's works provided new beneficial outlooks in the cement industry widened the understandings of cement chemistry and improved the notion of concrete durability [7].

Sulfate attack is defined as the deterioration of concrete involving any type of sulfate interactions with cement paste independently of the curing temperature and sulfate source [8]. This broad definition and implied focus on the sulfate ion may be misleading as to the type of attack investigated; whether it is delayed ettringite formation or external sodium sulfate attack [9]. The fact that the presence of ettringite may not be a sign of attack is emphasized by Skalny et al. [10] and supported by Neville [11]. On the other hand, according to ACIs there are two mechanisms that can be considered to be sulfate attack, formation of gypsum and formation of ettringite [12].

Portland cement-based materials subjected to attack from external sulfates may suffer from two types of damage, loss of strength of the matrix due to degradation of C–S–H, and volumetric expansion leading to cracking [13]. Loss of strength has been linked to decalcification of the cement paste hydrates upon sulfate ingress, especially C–S–H, or sulfate attack on C–S–H and CH in the presence of carbonate ions to form thaumasite. The thaumasite formation is accompanied by loss of strength and results in transformation of hardened concrete into a friable mass since a significant part of C–S–H can be destroyed. This process may occur with every type of sulfate salts and is encouraged by humid atmospheres and low temperature 10 °C [14]. Expansion, which leads to cracking, is attributed to the formation of expansive compounds such as ettringite. Three compounds may react with ingress sulfates, represented in the form of gypsum, according to one of the following reactions:

$$C_4AH_{13} + 3C\hat{S}H_2 + 14H \rightarrow C_6A\hat{S}_3H_{32} + CH \quad (1)$$

$$C_4A\hat{S}H_{12} + 2C\hat{S}H_2 + 16H \rightarrow C_6A\hat{S}_3H_{32} \quad (2)$$

$$C_3A + 3C\hat{S}H_2 + 26H \rightarrow C_6A\hat{S}_3H_{32} \quad (3)$$

These reactions are lumped in a global sulfate phase, aluminate phase reaction, as described in the literature [15] and represented as $Pi + ai\hat{S}$ to form $C_6A\hat{S}_3H_{32}$, where *Pi* represents the weighted average proportion of the aluminate phase taking part in the reaction, and *ai* represents the stoichiometric sulfate required for the reaction, namely, 3, 2, and 3 for Eqs. (1)–(3). Similar to the model by Clifton et al. (1994), the expansion is predicted from the molar volumes of the different components of the cement paste and its microstructure parameters, degree of hydration, and capillary porosity [16].

The primary manifestations of sulfate attack in cementitious materials visible to the naked eye include spalling, delamination, macrocracking and loss of cohesion. These are the consequences of complex chemical reactions and processes between the components of hydrated cement and sulfate compounds. Adsorption, desorption, dissolution or precipitation and recrystallization are some of the common types of reaction. Also sulfate generates deterioration in normal concrete including expansion, cracking, loss of stiffness, strength and sometimes disintegration. Solid sulfate salts does not attack concrete, but when present in solution, they react with the hardened cement [17,18].

Usually, alumina-bearing phases and calcium hydroxide are more vulnerable to sulfate attack than other elements present in hydrated Portland cement. The sulfate ions react with calcium hydroxide CH and calcium aluminate hydrate. The products of reactions are gypsum and calcium sulfo-aluminate (ettringite) has a considerably greater volume than the compounds that replace. Thus, the reactions with sulfate lead to expansion, causes internal stresses leading to disruption of the concrete [18]. The mechanism of expansion can be considered as follows: increase in solid volume, expansion in a topochemical reaction, oriented crystal growth, crystallization pressure, swelling phenomena, osmotic pressure, and reversal of local desiccation as shown in Fig. 1.

Available performance tests for evaluating sulfate resistance

The rapid mortar bar test (ASTM C452)

The rapid mortar bar test ASTM C452, the standard test method for potential expansion of Portland-cement mortars exposed to sulfate, was originally published and approved by ASTM C01.29, the subcommittee for sulfate resistance, in 1960. The test method involves the measurement of expansion of mortar bars made from a combination of Portland cement and gypsum. The gypsum in the mortar mix provides the source of sulfate that instigates rapid reaction in the specimens. The gypsum accelerates development and increases the amount of ettringite produced in the fresh and hardened concrete and accelerates the reactions typical of sulfate attack. The test method has referred to in the ASTM standards for Portland cement, ASTM C150. ASTM C150 designates a maximum expansion limit of 0.04% at 14 days for type V Portland cement. ASTM subcommittee C01.29 recommends limits of 0.06% expansion at 14 days for moderate sulfate resistant type II cement and 0.04% expansion at 14 days for severe sulfate-resistant type V cements.

The major advantage of ASTM C452 is the short duration of test. The sulfate resistance of mortar can be evaluated in

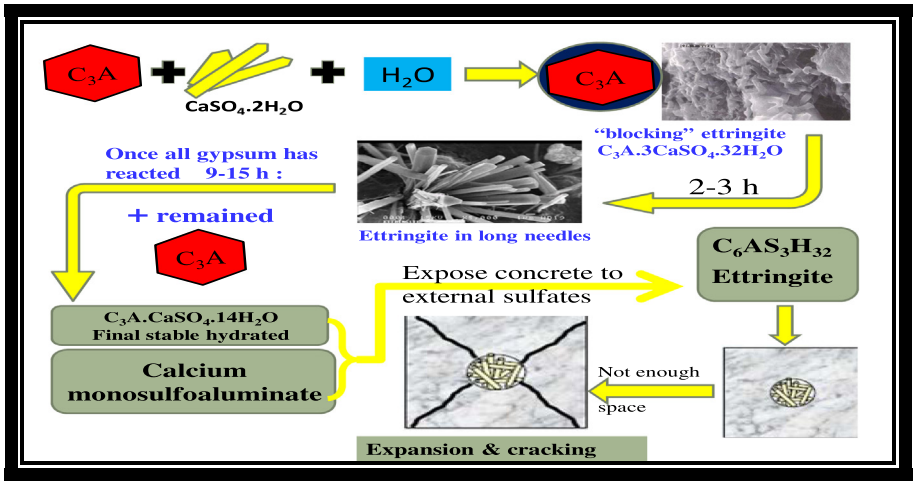

Fig. 1 Mechanism of sulfate attack (Fate of sulfate and calcium aluminates in normal hydration).

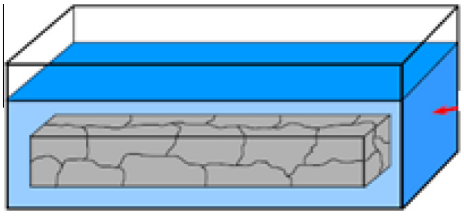

Fig. 2 ASTM C452 aggregate/cementitious material = 2.75 & W/CM = 0.485, gypsum added to produce 7% SO_3 by mass of cement + gypsum and Mortar bars ($25 \times 25 \times 250$ mm) then immersed in limewater replaced every 7 days for 28 days and every 28 days thereafter. Then expansion was monitored.

approximately 14 days. The major disadvantage of the test is that it has shown to be inaccurate when used for testing mortar made with blended hydraulic cement or blends of cement and a mineral admixture. The first problem is that the blended cement does not develop enough maturity in the 14 day measured expansion period. Secondly, the test does not represent field conditions because the gypsum incorporated into the mix exposes the mortar to sulfate attack in its fresh state before hydration has even occurred. The advantages of reduced potential for ettringite formation and lowered permeability are minimized. These flaws in the test have led researchers to limit the scope of ASTM C452. Fig. 2; shows the ASTM C452 technique.

ASTM C1012-95 standard test method for length change of hydraulic cement mortars exposed to a sulfate solution

ASTM subcommittee Co1.29 began researching the development of a new performance test that would be applicable to Portland cement and blends of Portland cement with pozzolans and slag. The result of this work was the formation and standardization of the mortar bar test, ASTM C1012, in 1984, as shown in Fig. 3. For the new test, the method of adding sulfate into the mortar during mixing is eliminated, sulfate exposure is provided by immersing the mortar bars in a sulfate solution after the mortar has reached certain strength. Beginning sulfate exposure when mortar at an equivalent strength value is said to simulate actual concrete, Practice in that concrete in the field will typically be at approximately the same strength when sulfate attack begins regardless of the cementation chemistry. The type of solution used for the test and the strength requirement has varied over the years, but the subcommittee has currently settled on using a 0.352 M sodium sulfate Na_2SO_4 solution and a strength requirement of 19.7 MPa before immersion.

Through analysis of test results and correlation with ASTM C452 limits, ASTM C01.29 was able to establish expansion criteria to correspond with the ASTM C1012 test. The test criterion requires a maximum expansion limit of 0.1% at 180 days of sulfate solution exposure for moderate sulfate resistance and a limit of 0.05% at 180 days for severe sulfate resistance.

However, there are deficiencies in this test method including lengthy measuring period (usually more than six months), insensitivity of the measurement tool to the progression of sulfate attack, the effect of curing (especially in the case of mineral admixture) and the effect of the pH change during the time in the solution [3–5]. The clear advantage of the test is that it provides a reliable way for engineers to evaluate the sulfate resistance of all types of cementation material combinations.

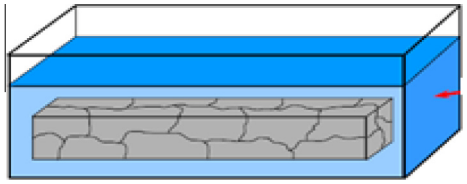

Fig. 3 ASTM C1012-95 aggregate/cementitious material = 2.75 & W/CM = 0.485, Mortars stored in limewater until a strength of 20 MPa is attained and Mortar bars ($25 \times 25 \times 250$ mm) then immersed in a 5% solution of sodium sulfate changed periodically for 6 months or 1 year and then length change monitored during storage.

Purpose of the present study

The aim of this study is to build a model in neural network systems, this model simulates the ASTM C1012-95 standard test method for length change of hydraulic cement mortars exposed to a sulfate solution. Moreover to recover the deficiencies in the ASTM C1012-95 test method as mentioned above, also to study the role of incorporation of the mineral admixture characteristics of concrete and to assess the effect of exposure duration on the performance of concrete when exposed to sulfate attack, moreover, to investigate the effect of initial conditions of the problem, such as chemical composition of the cement and C_3A content.

Background of neural network

Neural networks are composed of simple elements operating in parallel. These elements are inspired by biological nervous systems. As in nature, the network function is determined largely by the connections between elements. We can train a neural network to perform a particular function by adjusting the values of the connections (weights) between elements. Commonly neural networks are adjusted, or trained, so that a particular input leads to a specific target output. Such a situation is shown in Figs. 4 and 5. There, the network is adjusted, based on a comparison of the output and the target, until the network output matches the target [19].

Certain kinds of linear networks and Hopfield networks are designed directly. In summary, there are a variety of kinds of design and learning techniques that enrich the choices that a user can make. The field of neural networks has a history of some five decades but has found solid application only in the past fifteen years, and the field is still developing rapidly. Thus, it is distinctly different from the fields of control systems or optimization where terminology, basic mathematics, and design procedures have been firmly established and applied for many years [19].

An overview study on neural network algorithms is provided by McCulloch and Pitts [20]. A neuron as a unit with the process of stimulus and reaction is generalized in this system. The training for learning a set of data is performed with weight (connection strength), transfer function, and biases. The error between calculated results and expected results is decreased with increasing epochs and training for learning is finished within a target convergence. In this study, a back-propagation algorithm is used for developing a more rapid modeling to assess the sulfate resistance of hydraulic cements.

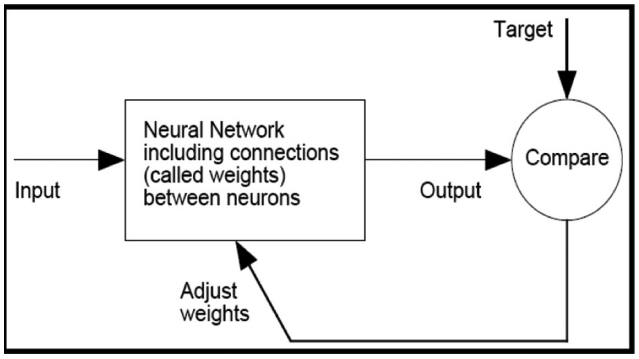

Fig. 4 Outline of simple neural network architecture.

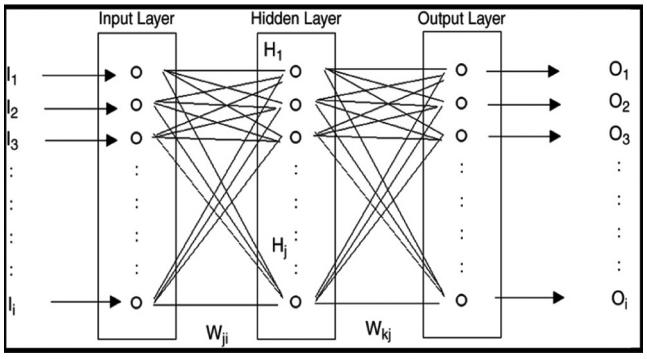

Fig. 5 Outline of simple neural network architecture.

For the last two decades, the different modeling methods based on artificial neural networks (ANN) systems have become popular and has been used by many researchers for a variety of engineering applications. The basic strategy for developing ANN system based models for material behavior is to train ANN on the results of a series of experiments using that material. If the experimental results contain the relevant information about the material behavior, then the trained ANN will contain sufficient information about material's behavior to qualify as a material model. Such a trained ANN system not only would be able to reproduce the experimental results, but also they would be able to approximate the results in other experiments through their generalization capability [21].

Neuron model and transfer functions

A neuron with a single scalar input and no bias appears on Fig. 6. The scalar input p is transmitted through a connection that multiplies its strength by the scalar weight w, to form the product wp, again a scalar. Here the weighted input wp is the only argument of the transfer function f, which produces the scalar output a. The neuron on the Fig. 7 has a scalar bias, b. You may view the bias as simply being added to the product wp as shown by the summing junction or as shifting the function f to the left by an amount b. The bias is much like a

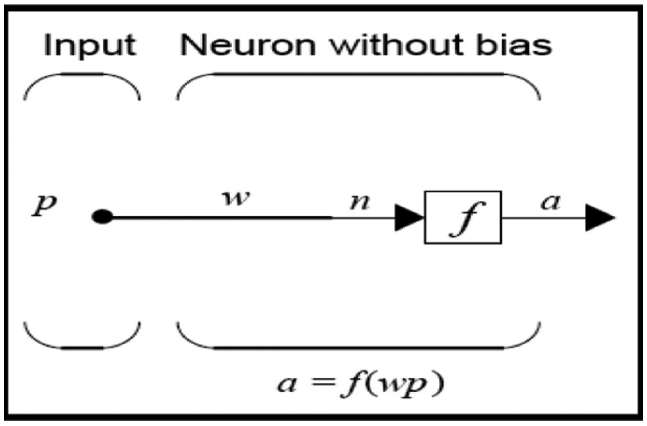

Fig. 6 A neuron with a single scalar input without bias.

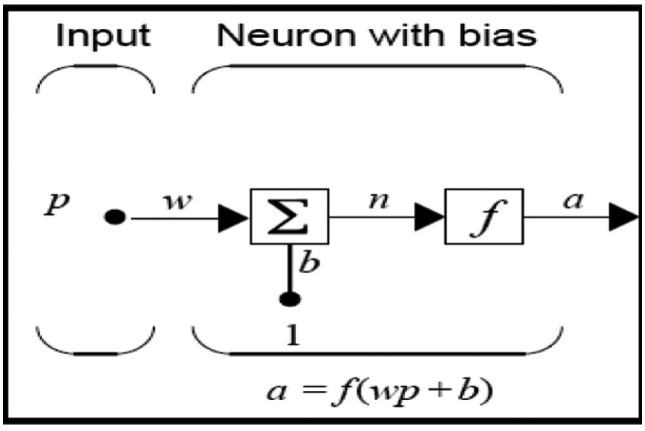

Fig. 7 A neuron with a single scalar input and a scalar bias.

weight, except that it has a constant input of 1. The transfer function net input n, again a scalar, is the sum of the weighted input wp and the bias b. This sum is the argument of the transfer function f. Here f is a transfer function, typically a step function or a sigmoid function, which takes the argument n and produces the output a. Examples of various transfer functions are given in the next section. Note that w and b are both adjustable scalar parameters of the neuron. The central idea of neural networks is that such parameters can be adjusted so that the network exhibits some desired or interesting behavior. Thus, we can train the network to do a particular job by adjusting the weight or bias parameters, or perhaps the network itself will adjust these parameters to achieve some desired end.

A neuron with a single R-element input vector is shown in Fig. 8 where R = number of elements in input vector. Here the individual element inputs p_1, p_2, …, p_R are multiplied by weights $w_{1,1}$, $w_{1,2}$, …, $w_{1,R}$ and the weighted values are fed to the summing junction. Their sum is simply Wp, the dot product of the (single row) matrix W and the vector p. The neuron has a bias b, which is summed with the weighted inputs to form the net input n. This sum, n, is the argument of the transfer function f. $n = w_{1,1}\,p_1 + w_{1,2}\,p_2 + \cdot\ + w_{1,R}\,p_R + b$.

Many transfer functions are included in ANN. Three of the most commonly used functions are shown in Fig. 9. The hard-limit transfer function limits the output of the neuron to either 0, if the net input argument n is less than 0; or 1, if n is greater than or equal to 0. The linear transfer function, Neurons of this type is used as linear approximators in "Linear Filters". The sigmoid transfer function takes the input, which may have any value between plus and minus infinity, and squashes the output into the range 0–1. This transfer function is commonly used in backpropagation networks, in part because it is differentiable. The symbol in the square to the right of each transfer function graph shown below represents the associated transfer function. These icons will replace the general f in the boxes of network diagrams to show the particular transfer function being used.

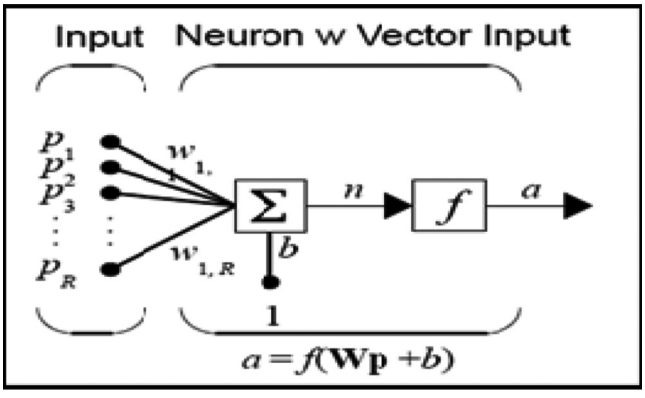

Fig. 8 A neuron with a single R-element input vector.

Previous studies via ANN

In recent years ANN can be trained to solve problems that are difficult for conventional computers or human beings. ANN has been applied to many other fields, Aerospace, Automotive, Banking, Credit Card Activity Checking, Defense, Electronics, Entertainment, Financial, Industrial, Insurance, Manufacturing, Medical, Oil and Gas, Robotics, Speech, Securities, Telecommunications, Transportation, and Civil engineering [22]. Today, ANN has been applied to many civil engineering problems with some degree of success, as, detection of structural damage, structural system identification, modeling of material behavior, structural optimization, structural control, ground water monitoring, prediction of settlement of shallow foundation, concrete mix proportions, and predicting properties of conventional concrete and high performance concretes [22–26].

Dias and Pooliyadda (2001) used back propagation neural networks to predict the strength and slump of ready mixed concrete and high strength concrete, in which chemical admixtures and/or mineral additives were used. According to the authors, the neural network models also performed better than the multiple regression ones, especially in reducing the scatter of predictions [27].

Oztas et al. (2006) studied with the ANN for developing a methodology for predicting compressive strength of HSC with suitable workability. They arranged to the data used in the ANN model in a format of seven input parameters that cover the water-to-binder ratio, water content, fine aggregate ratio, fly ash content, air entraining agent content, and silica fume replacement. The proposed ANN model predicts the compressive strength and slump value of HSCs.

Baykasoglu et al. (2004) used the soft computing techniques which were gene expression programing and neural networks, for predicting the 28 day compressive strength of Portland composite cement. Besides, they used the stepwise regression analysis to have an idea about the predictive power of the soft computing techniques in comparison to the classical statistical approach [28].

Pala et al. (2005) focused on studying the effects of fly ash and silica fume replacement content on the strength of concrete cured for a long term period of time by using neural networks. The NN model arranged was composed of eight input parameters that cover the fly ash replacement ratio, silica fume replacement ratio, and total cementitious material, fine aggregate, coarse aggregate, water content, high rate water reducing agent and age of samples and an output parameter that is compressive strength. The authors explained that NNs have strong potential as a feasible tool for evaluation of the effect of cementitious material on the compressive strength of concrete [29].

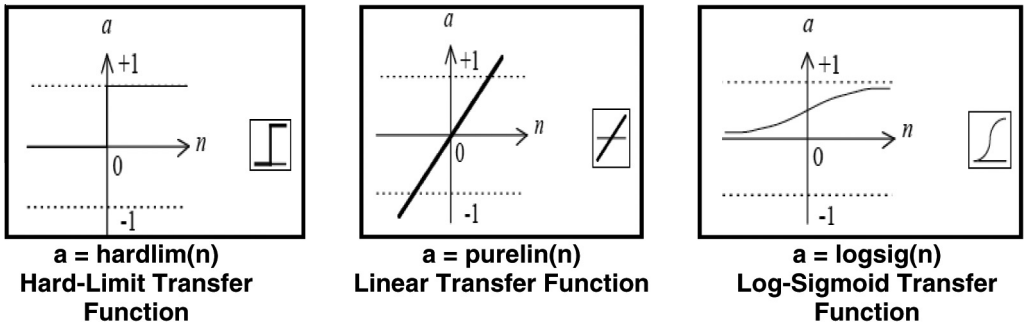

Fig. 9 Three of the most commonly used functions.

Design, training and testing of neural networks modeling

To design and build model in neural network systems, this model to simulate ASTM C1012-95, cement type, cement content, two types of mineral admixture, and duration, were taken as the five input parameters and the output parameter was taken as the expansion.

The ANN models designed according to these parameters are shown in Fig. 10. Neuron numbers in the hidden layer were tested for different values and a network of two neurons were chosen as it yielded the most appropriate result.

For the purpose of constructing this model, 16 different mixes with 48 mortar bar specimens, 112 length measurements were taken at 7, 14, 21, 30, 56, 90, 105, days after the bars were initially placed in the sodium sulfate solution. 32 Long term measurements were taken after 120 and 180 days of soaking. The expansion after 180 days of soaking is the critical measurement because this value is used as a criterion for determining sulfate resistance. Experimental results of cement mortar mixes used in training and testing the model were gathered from the technical literature.

Plain Portland cement mortars, mortars with cement combined with fly ash, and mortars with cement combined with slag were tested by using ASTM C1012-95. Four cements, with tow ratio of fly ash, and one ratio of ground granulated blast furnace slag (GGBFS) were obtained from the literature. One ASTM C150 type I, two type I–II and type V Portland cement were tested. Four material combinations were evaluated for each cement. The cementation material combinations considered for each cement are four mixes by four types of cement only, eight mixes by combined tow ratio of Class F fly ash with four types of cement and four mixes by combined 50% volumetric replacement of slag with four types of cement.

In the training of the models; duration in day (D), type of Portland cement function of C_3A content 12%, 5.1%, 7%, and 0% equivalent to type I, I–II(A), I–II(B), V, respectively, cement content (CC), fly ash Class F 20% (F1), fly ash Class F 30% (F2), GGPFS 50% (S) were entered as input parameters while expansion (E) was used as output. The models were trained with 144 input data obtained from available experimental results. The following Tables (1–4) provide the mix proportions of Type I cement mortars and the relevant experimental measurements. Tables 5–7 provide the relevant information for other studied mortar mixes.

Limitation of the experimental result chosen from the literature and meeting the requirements of ASTM C1012-95

The following sections provide information on the materials and mix proportions, test techniques and procedures used in the mortar mixes for this modeling. The Portland cements, fine aggregate and mineral admixtures are described and potable water was used for all mixing.

Portland cement

Four commercially available Portland cements were evaluated in this modeling, one type I, two type I–II A&B and type V cement. Chemical analyses for the four cements are provided in Table 5. A specific gravity of 3.15 was assumed for proportioning for all the cements. Type I cement has no ASTM C150 limit for C_3A content, thus the high 12% value is acceptable. Type I–II (A) cement has a C_3A content of 5.1%. This value is considerably lower than the ASTM C150 maximum limit of 8% for type II cement and is just above the 5% limit required for Type V cement. The 7% C_3A content of the type I–II(B) cement is just below the ASTM C150 limit of 8% for type II cement. Finally, Type V cement meets the C_3A content limit of 5% for sulfate resistant cement because the cement contains zero C_3A.

Fine aggregate

The fine aggregate used for making the mortar was a graded sand meeting the requirements of ASTM C778-97. ASTM C1012-95 requires that mortar for this test be made with this

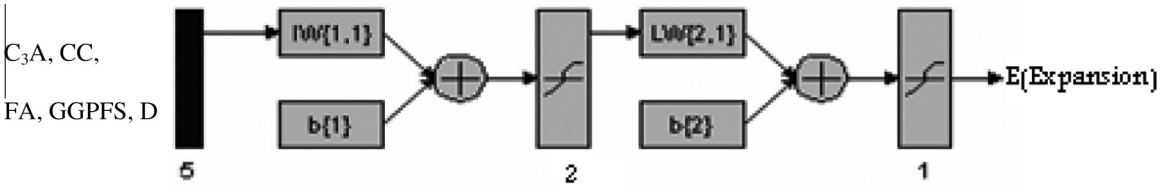

Fig. 10 The model of ANN designed.

Table 1 PI type I cement only.

Cement type (C_3A)	0.12	0.12	0.12	0.12	0.12	0.12	0.12	0.12	0.12
Cement content (CC)/1000	0.532	0.532	0.532	0.532	0.532	0.532	0.532	0.532	0.532
Fly ash Class F (F)	0	0	0	0	0	0	0	0	0
GGBF slag (S)	0	0	0	0	0	0	0	0	0
Duration (D) year = 360 day	0.0194	0.039	0.058	0.077	0.155	0.25	0.291	0.333	0.5
Expansion (E)%	0.007	0.011	0.013	0.017	0.019	0.032	0.037	0.074	0.199

Table 2 PI-F1 type I cement and 20% fly ash CaO < 25%.

Cement type (C_3A)	0.12	0.12	0.12	0.12	0.12	0.12	0.12	0.12	0.12
Cement content (CC)/1000	0.425	0.425	0.425	0.425	0.425	0.425	0.425	0.425	0.425
Fly ash (FA-1)%	0.2	0.2	0.2	0.2	0.2	0.2	0.2	0.2	0.2
GGBF slag (S)	0	0	0	0	0	0	0	0	0
Duration (D) year = 360 day	0.019	0.039	0.058	0.077	0.155	0.25	0.291	0.333	0.5
Expansion (E)%	0.004	0.008	0.01	0.012	0.017	0.02	0.024	0.024	0.028

Table 3 PI-F2 type I cement and 30% fly ash CaO < 25%.

Cement type (C_3A)	0.12	0.12	0.12	0.12	0.12	0.12	0.12	0.12	0.12
Cement content (CC)/1000	0.372	0.372	0.372	0.372	0.372	0.372	0.372	0.372	0.372
Fly ash Class F (FA)%	0.3	0.3	0.3	0.3	0.3	0.3	0.3	0.3	0.3
GGBF slag (S)	0	0	0	0	0	0	0	0	0
Duration (D) year = 360 day	0.019	0.039	0.058	0.077	0.155	0.25	0.291	0.333	0.5
Expansion (E)%	0.003	0.006	0.01	0.011	0.022	0.029	0.03	0.037	0.045

Table 4 PI S type I cement and 50% GGBF slag.

Cement type (C_3A)	0.12	0.12	0.12	0.12	0.12	0.12	0.12	0.12	0.12
Cement content (CC)/1000	0.266	0.266	0.266	0.266	0.266	0.266	0.266	0.266	0.266
Fly ash Class F (FA)%	0	0	0	0	0	0	0	0	0
GGBF slag (S)	0.5	0.5	0.5	0.5	0.5	0.5	0.5	0.5	0.5
Duration (D) year = 360 day	0.019	0.039	0.058	0.077	0.155	0.25	0.291	0.333	0.5
Expansion (E)%	0.004	0.008	0.012	0.012	0.017	0.023	0.023	0.033	0.038

Table 5 Chemical and physical properties for cement. (EA = Equivalent Alkalies).

Cement type (ASTM C150)	%										
	SiO_2	Al_2O_3	Fe_2O_3	MgO	SO_3	E A	LOI	IR	C_2S	C_3S	C_3A
I	20.6	5.07	2.09	1.3	3.5	0.64	1.8	0.16	14	61	12
I–II(A)	20.42	4.42	3.94	1.06	2.96	–	0.76	0.13	11.7	62.1	5.1
I–II(B)	20.9	4.5	3.2	1.4	3	0.43	1.3	0.15	–	61	7
V	21.86	3.18	5.66	0.75	3.06	0.38	0.67	–	21.8	54.2	0

well-graded, rounded particle sand. The sand is predominately graded between 600 μm (No. 30) and 150 μm (No. 100) standard sieve sizes such that a very fine, well-distributed aggregate is created. The sand has a specific gravity of 2.65 and an absorption capacity of 0.5%.

Mineral admixtures

Two different types of mineral admixture were chosen in mixes to build the model, a low-calcium ASTM Class F fly ash, and a ground granulated blast furnace slag. The chemical and physical properties of the mineral admixtures are shown in Table 6. The relevant chemical components for the fly ashes regarding sulfate attack of concrete are calcium oxide (CaO), silicon dioxide (SiO_2), aluminum oxide (Al_2O_3), and iron oxide (Fe_2O_3) components.

Mix proportioning and test techniques

The mix proportioning for the mortar is as required by ASTM C1012-95. Proportioning consisted of adding one part cement to 2.75 parts graded standard sand by weight. For the plain Portland cement mortar, the procedures require a water to cement ratio of 0.485 for non air entrained cement. The basic mix proportions for the plain Portland cement mortars are 265 kg/m^3 water, 532 kg/m^3 Portland cement and

Table 6 Chemical and physical properties of mineral admixtures.

Mineral admixture	SiO_2	Al_2O_3	Fe_2O_3	CaO	MgO	SO_3	S	LOI	Moi. Con.	Ret. #325 sieve	SG
ASTM Class F fly ash	47.8	22.6	5.9	4.56	2.3	0.7	–	0.1	0.1	0	2.53
GGBF slag	32.74	13.23	0.41	44.14	5.62	1.48	1.3	0.2	0.13	62.1	2.86

Table 7 Description, mix condition, and fresh properties of modeling mortar.

Batch name	Cement type	F ash/slag (% Rep)	Mix temp. (°C)	Relative humidity (%)	Water (kg/m^3)	Cement content (kg/m^3)	F ash/slag (kg/m^3)	Flow number
PA	I–II(A)	None	22.2	63	265	523	0	105
PA-F1	I–II(A)	F (20%)	22.77	65	262	425	85	107.5
PA-F2	I–II(A)	F (30%)	22.2	66	258	372	128	117.5
PA-S	I–II(A)	Slag (50%)	21.66	65	278	266	241	105.5
PB	I–II(B)	None	22.2	62	265	523	0	107.5
PB-F1	I–II(B)	F (20%)	22.77	65	261	425	85	106
PB-F2	I–II(B)	F (30%)	22.2	67	258	372	128	113
PB-S	I–II(B)	Slag (50%)	23.88	67	279	266	241	114.5
PV	V	None	23.88	65	265	523	0	97.5
PV-F1	V	F (20%)	22.2	62	263	425	85	112
PV-F2	V	F (30%)	22.77	62	260	372	128	114.5
PV-S	V	Slag (50%)	23.88	65	284	266	241	116
PI	I	None	22.77	63	265	523	0	120
PI-F1	I	F (20%)	21.66	63	260	425	85	121.5
PI-F2	I	F (30%)	21.11	62	257	372	128	119.5
PI-S	I	Slag (50%)	21.11	60	274	266	241	123

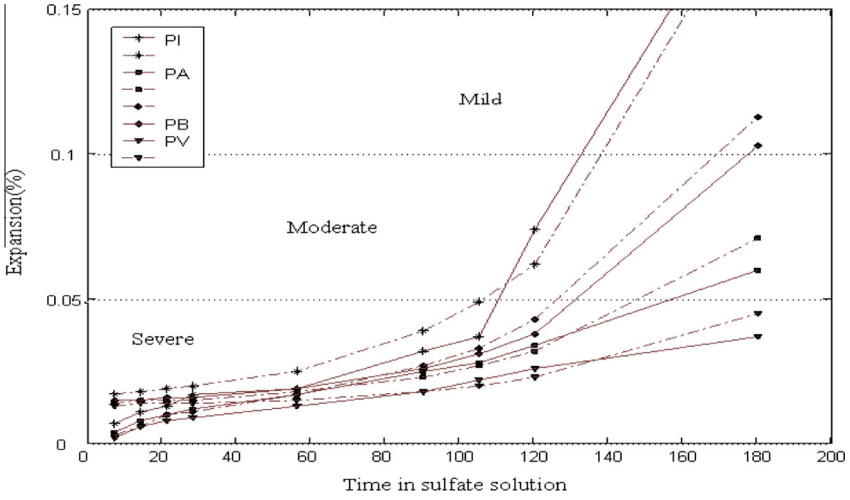

Fig. 11 Sulfate expansion of plain Portland cement mortar.

1456.5 kg/m^3 for sand, details for all the mixes performed for built model are provided in Table 7. The air content for the mortar was assumed to be 2%. The water content is based on the assumption that the sand is completely dry at the time of mixing and the sand has absorption of 0.5%.

When mineral admixtures were used, a specified volumetric percent of the cement was replaced by an equivalent volume of the mineral admixture. The Class F fly ash was used to replace 20% and 30% of the cement. And the slag was used to replace 50% of the cement. For mortars with these blends of Portland cement with fly ash or slag, the required water to cementations material ratio was designated in two manners. ASTM C1012-95 states the water to cementation material ratio shall develop a flow within ± 5 of the flow number found for the plain Portland cement mortars with a 0.485 w/c ratio. Also ASTM C1012-95 refers to the ASTM C109-95 procedures where it is recommended that the water to cementation material ratio produce a flow number within the range of 110 ± 5. For this build of the model, the goal was to meet both these requirements when possible to ensure the mortar with admixtures compared well with their plain Portland cement mortar control as well as with all the other mortars used in the build of the model.

ASTM C1012-95 designates the ASTM C684-95 procedure (warm-water method) for initial curing of the mortar

Table 8 180 Day expansion for plain Portland cement mortar, experimental and simulate.

Batch name	Cement type	C_3A content (%)	%180 day Expansion experimental	%180 day Expansion simulating
PA	I–II A	5.1	0.06	0.083
PB	I–II B	7	0.113	0.103
PV	V	0	0.037	0.04
PI	I	12	0.199	0.195

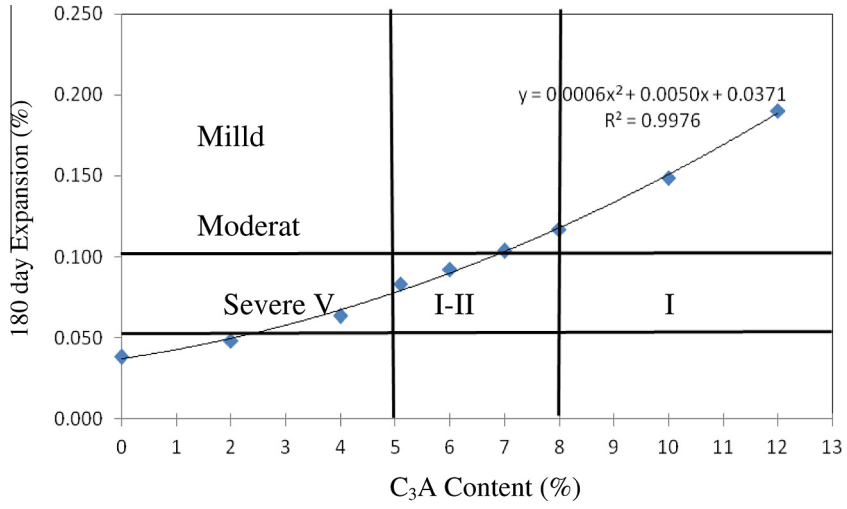

Fig. 12 180 Day expansion versus cement C_3A content for plain Portland cement mortar.

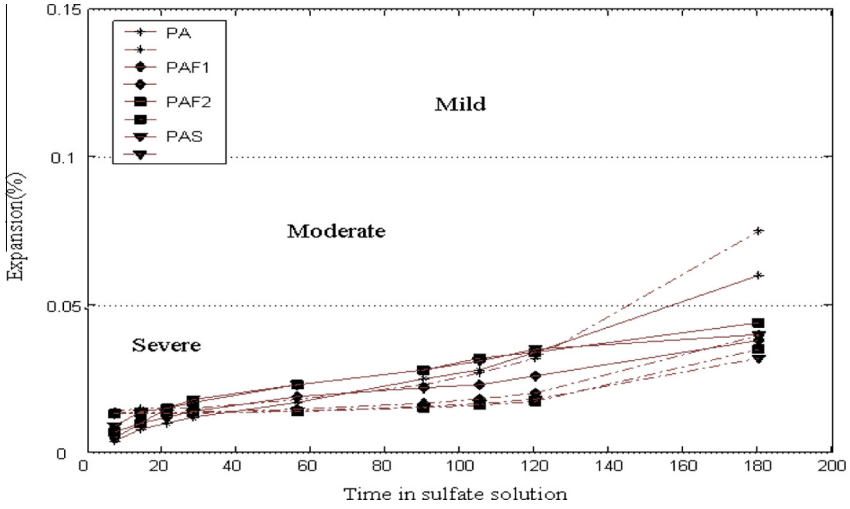

Fig. 13 Sulfate expansion of mortar containing combination of type I–II(A) cement with mineral admixtures.

specimens after placement. The procedure involves sealing the top of the molds with a rigid steel, glass, or plastic plate such that the mold is completely watertight. The molds are then immersed in a curing tank of water that is kept at 35 ± 3 °C. The molds are kept in the tank for 23.5 ± 0.5 h. The results of early research work suggested modifying the procedure so that specimens were stored in 100% relative humidity environment instead of being submerged in a tank. Attempting to create a completely watertight mold proved to be time consuming and risky because a leak in the mold would result in loss of the specimens. The modified procedure involved placing the mortar specimens in an environmental chamber that was kept at 35 ± 3 °C. The molds were covered with moist cloths and then sealed in plastic bags. Water trays were also placed inside the chamber to keep the humidity high. All these steps were done to ensure a 100% relative humidity environment was produced so that the fresh mortar did not lose any water. Creating this environment serves the same purpose as immersing the specimens in a curing tank. The molds were kept in the chamber for 23.5 ± 5 h.

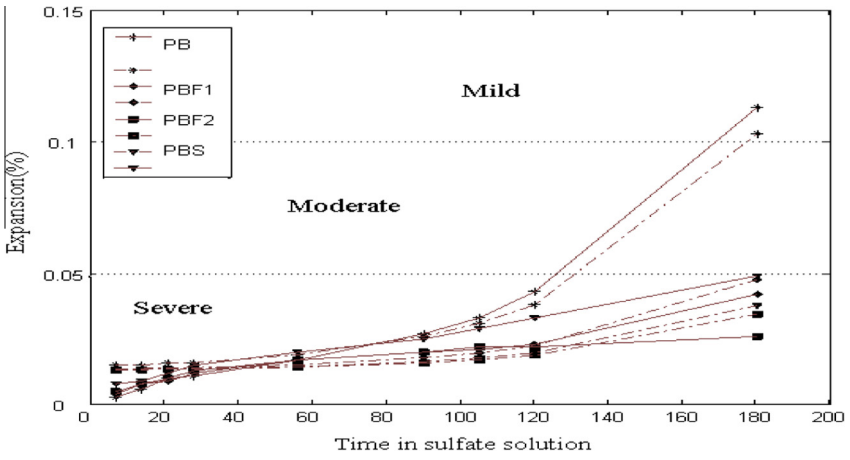

Fig. 14 Sulfate expansion of mortar containing combination of type I–II(B) cement with mineral admixtures.

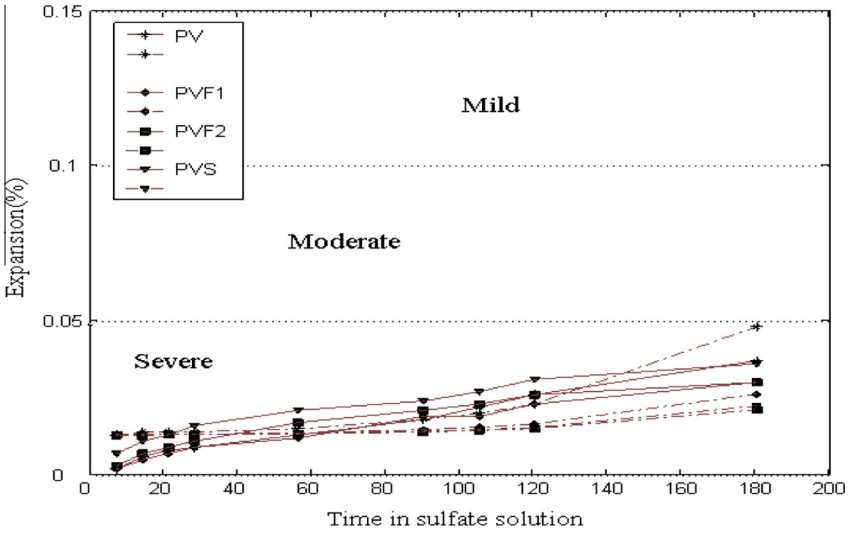

Fig. 15 Sulfate expansion of mortar containing combination of type I–II(B) cement with mineral admixtures.

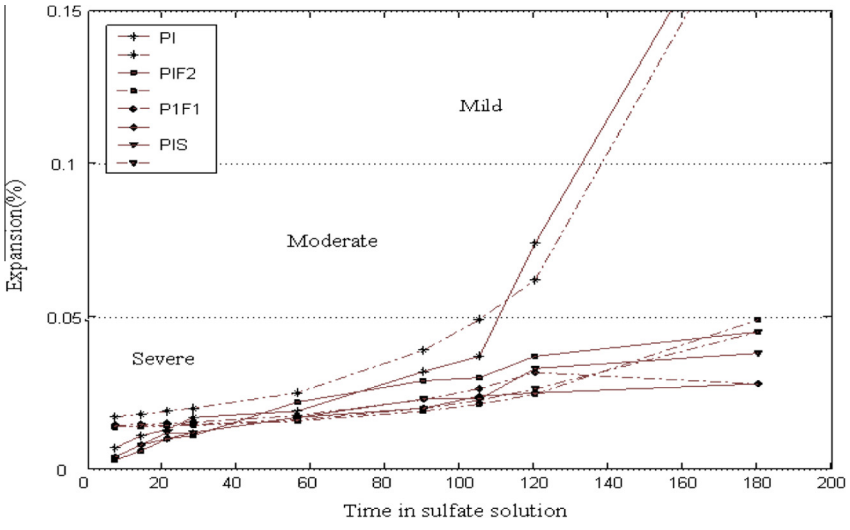

Fig. 16 Sulfate expansion of mortar containing a combination of type I cement with mineral admixtures.

Table 9 180 Day expansion for mortar containing combination of type I–II(A) cement with mineral admixtures, experimental and simulate.

Batch name	FA/slag	Rep (%)	%180 day Expansion experimental	%180 day Expansion simulating
PA	None	0	0.060	0.065
PA-F1	FA	20	0.038	0.039
PA-F2	FA	30	0.044	0.037
PA-S	Slag	50	0.040	0.035

Table 10 180 Day expansion for mortar containing combination of type I–II(B)cement with mineral admixtures, experimental and simulate.

Batch name	FA/slag	Rep (%)	%180 day Expansion experimental	%180 day Expansion simulating
PB	None	0	0.113	0.103
PB-F1	FA	20	0.041	0.045
PB-F2	FA	30	0.026	0.037
PB-S	Slag	50	0.049	0.038

Table 11 180 day Expansion for mortar containing combination of type V cement with mineral admixtures, experimental and simulate.

Batch name	FA/slag	Rep (%)	%180 day Expansion experimental	%180 day Expansion simulating
PV	None	0	0.037	0.047
PV-F1	FA	20	0.030	0.032
PV-F2	FA	30	0.030	0.037
PV-S	Slag	50	0.036	0.039

Table 12 180 day Expansion for mortar containing combination of type I cement with mineral admixtures, experimental and simulate.

Batch name	FA/slag	Rep (%)	%180 day Expansion experimental	%180 day Expansion simulating
PI	None	0	0.199	0.195
PI-F1	FA	20	0.028	0.0278
PI-F2	FA	30	0.045	0.037
PI-S	Slag	50	0.038	0.048

After initial length measurements, the mortar bars were immediately immersed in a sodium sulfate solution. The bars were stored in containers with lids so that the solution would not evaporate. The bars were supported by several 13 mm diameter PVC pipes so that no surface of the bars touched any side of the container. Following test requirements, the sodium sulfate solution was prepared at least 1 day before its use. The solution designated by ASTM C1012-95 was a 0.352 M, 5% sodium sulfate (Na_2SO_4) solution. One liter of solution was prepared by first dissolving 50.0 g of anhydrous technical grade Na_2SO_4 salt in 900 mm of deionized water. After the salt was dissolved, the solution was diluted to 1 L by adding deionized water. The solution was required to have a pH between 6 and 8. Throughout all the testing, the sodium sulfate solutions were kept at 23 ± 1 °C. ASTM C1012-95 requires that the mortar bars be stored such that a sulfate solution to bar volume ratio of 4 ± 0.5 exists.

Simulation results and analysis

Model calibration and validation standard with respect to ASTM C1012-95 test

A quite high correlation was found between the results of experimental ASTM C1012-95 test and the simulation resulting of modeling by ANN via ANN modeling data, it can be suggested that ANN can reliably predict the value of the expansion of mortar bar. These values remained within the

range of the experimental ASTM C1012-95 test found in previous studies which used to simulate and determine the value of expansion.

Sulfate expansion results for plain Portland cement mortars

In addition, the analysis was made between sulfate expansions of plain Portland cement mortars with different values of C_3A content obtained from literature experimental data (denoted by solid line) and the numerical results from training the model (denoted by dash line). The resulting graphical relation is presented in Fig. 11 and the values are compared in Table 8.

Fig. 11 shows comparing between experimental and simulation data bar expansion after 1, 2, 3, 4, 8, 13 and 15 weeks and 4 months (120 days) and 6 months (180 days) of continuous soaking in sodium sulfate solution. For each mortar, the expansion limits defined for ASTM C1012-95 tests are depicted graphically in the figure by a horizontal gridline. According to the limits, mortars having 180-day expansion of less than 0.05% meet the requirements for a severe sulfate environment, mortars with a 180-day expansion of 0.10 or less meet the requirements for a moderate sulfate environment, and mortars with 180-day expansions exceeding 0.1% are only applicable in mild environments.

The mortar bars containing the type I–II(A) cement had 180-day expansion slightly above 0.05% for both experimental and numerical results. A 180-day expansion of 0.06%, 0.083% was obtained for the mortar. The type I–II(B) cement mortar had higher expansions exceeding 0.10% at 180 days, the 180-day expansion for the mortar was 0.113%, 0.103% for both experimental and numerical data respectively. The mortar mix PV for type V cement had the lowest 180-day expansion; 0.037%, 0.04% for both expansions of experimental and numerical data respectively, were well below 0.05%. The mortar mix PV for type V cement had the lowest 180-day expansion; 0.037%, 0.04% for experimental measurements and numerical simulations; respectively. These values are well below the 0.05% limit. Mortar mix PI, containing type I cement had the highest expansions of plain portland cement mortars as its 180-day expansion reached 0.199% (experimental measurements) and 0.195% (numerical simulatio).

Generally, the numerical results are in good agreement with experimental data. Some numerical data show more 180 day expansion than experimental data and it is expected that a slightly higher expansion is obtained in accelerated modeling but this slightly different not cause any change in the category of cement according to the expansion limits defined for ASTM C1012-95.

Effects of cement chemistry on sulfate resistance and examinants the modeling

As discussed in introduction, past research has established that the most important Portland cement chemical component affecting sulfate resistance is the tricalcium aluminate C_3A content of the cement. To examinants the modeling by nine types of cement with different C_3A content ranging from 0% to 12% was trained. Fig. 12 provides a plot of the numerical results of 180-day expansions that were obtained for the nine plain Portland cement mortars versus the C_3A content of the cements used in the industrial concrete.

The horizontal gridlines in Fig. 12 represent the ASTM C1012-95 expansion limits and proposed in this modeling performance based specifications. The line at 180-day expansion of 0.1% delineates between mild and moderate sulfate environment resistance while the line at an expansion of 0.05% delineates between moderate and severe sulfate resistance. The vertical gridlines represent the Portland cement C_3A content limits established in the ASTM C150 specifications for categorizing sulfate resistant cement. A line is provided at 5% C_3A to represent the maximum allowable C_3A content of severe sulfate resistance type V cement, and another line is provided at 8% to represent the maximum allowable content for the moderate sulfate resistant type I–II or type II cements.

The numerical results from training the model equivalent to ASTM C1012-95 confirmed the well-supported fact that the C_3A content of cement greatly impacts its sulfate resistance. The second degree polynomial trend line shown in Fig. 12 displays a clear increase in expansion and thus a decrease in sulfate resistance as the cement C_3A content increased. The rate of expansion increased as the C_3A contents increased.

In comparing the levels of sulfate resistance determined for training and simulation of model using the ASTM C1012-95 expansion criteria versus the ASTM C150 C_3A content limits, the type I cement was found to be only adequate in mild sulfate environments according to the modeling of ASTM C1012-95 because of its high 180-day expansion of 0.195% and according to ASTM C150 because of its high C_3A content of 12%. The type V cement proved to be adequate for severe sulfate environments according to ASTM C1012-95 because its 180-day expansion was a low 0.037% and according to ASTM C150 because of its C_3A content of 0%. The type I–II(A) cement met the requirements for moderate sulfate environments according to ASTM C1012 because of its 180-day expansion of 0.083% and according to ASTM C150 because of its C_3A content of 5.1%.

Sulfate expansion results for mortars with mineral admixtures

Figs. 13–16 and Tables 9–12 present the experimental and numerical expansion results for the mortars containing combinations of cement with a mineral admixture. A figure is provided for each cement presenting the expansion for the three mortars with different cement–mineral admixture combinations. The expansion for the plain Portland cement mortar is also presented in each figure such that an observation can be made as to whether the mineral admixture increased or decreased sulfate resistance.

The effect of mineral admixtures had on the sulfate resistance of mortars varied depending on the cement with which they were blended. In general, all mortar mixes containing the ASTM Class F fly ash and the GGBFS slag all had average 180-day bar expansions below 0.05% for both experimental and numerical expansion results.

For type I–II(A) cement mortars, the addition of class F fly ash and GGBFS significantly reduced the 180-day expansion was reduced 26–33% in comparison with expansion of plain type I–II(A) cement mortars. It is noteworthy to report that the proposed ANN model captured the experimentally proven changes in the expansion performance of the different mortar types as a result of changing the fly ash replacement percentage.

The 180 day expansion reductions by the Class F fly ash and the slag were even greater for mortars containing the type I–II(B) cement as 0.113% a 180 day expansion of the plain Portland cement mortar was reduced 56 to 76%. The PB-F1 mix containing a 20% volumetric replacement of Class F fly ash reduced the plain cement mortars' 180 day expansion 64% to an average of 0.041%. This relation is true for both experimental and numerical expansion results regardless of the smallest difference in the value between experimental and numerical by modeling.

The reduction in 180 day expansions provided by the Class F fly ash and slag were relatively small when the admixtures were used in combination with the type V cement with 20% Class F fly ash replacement, Mix PV-F2 with a 30% fly ash replacement showed the same improvement as the same average 180 day expansion was obtained. The mix containing the slag PV-S, provided little improvement.

The most drastic level of reductions in sulfate expansions provided by the Class F fly ash and slag came when the admixtures were used with the type I cement. The PI-F1 with a 20% Class F fly ash replacement provided the greatest improvement as a 180 day expansion of 0.028% was obtained. This was a reduction of 86% from the expansion found for the plain cement mortar. The PI-F2 mix with a 30% Class F fly ash reduced expansions 77% as a 180 day average expansion of 0.045% was obtained. The slag mix, PA-S, reduced expansions of 81% as a 180 day average expansion of 0.035% was measured.

Conclusions

The ultimate goal of the training model was to determine the suitability of it as a performance modeling for evaluating the sulfate resistance of Portland cement and Portland cement mineral admixture combination. The modeling can be evaluated by investigating the consistency and thus the reliability of results obtained from the training model, correlation of the training model result with mortar experience in the concrete industry, accuracy and effectiveness of the modeling expansion result criteria used for determining the level of sulfate resistance of mortar.

The conclusions of this study are as follows.

1. The prediction modeling technique for analyzing the effects of cement types and mineral admixture on the sulfate attack with time-dependent value of expansion obtained from neural network algorithm is developed. Through the comparison of experimental data and numerical simulation results, a quite high correlation was found between the results of experimental ASTM C1012-95 test and the result of modeling by ANN via ANN modeling data, it can be suggested that ANN can reliably predict the value of the expansion of mortar bar.
2. It is shown that expansion in mortar bar can be estimated successfully through neural network algorithm having two neurons, which are five components in mixture design and duration time submerged condition. For 144 data-set of expansion, the average of difference between estimated results from neural network and from experimental data is evaluated to be 5%.
3. By utilizing more extensive and quantitative data-set considering mineral admixtures, time duration, and a large number of test specimens, this proposed technique on neural network algorithm can be more effective for evaluation of the effects of cement types and mineral admixture on the sulfate attack.
4. Sulfate expansion of ASTM C1012 modeling- training Portland cement mortar confirmed the impact the cement tricalcium aluminate C_3A content has on sulfate resistance as increasing C_3A content yielded increased expansion.

References

[1] R. Tixier, B. Mobasher, Modeling of damage in cement based materials subjected to external sulfate attack Part 1: Formulation, ASCE J. Mater. Eng. 15 (4) (2003) 305–313.
[2] Standard test method for length change of hydraulic cement mortars exposed to sulfate solution, ASTM C1012-04, vol. 04.01p.
[3] J.R. Clifton, G. Frohnsdorff, C. Ferraris, Standards for evaluating the susceptibility of cement based materials to external sulfate attack, Material Science of Concrete, Sulfate Attack Mechanisms, special volume, American Ceramic Society, 1999, pp. 337–355.
[4] C. Ferraris, P. Stutzman, M. Peltz, J. Winpigler, Developing a more rapid test to assess sulfate resistance of hydraulic cement, J. Res. Natl. Inst. Stand. Technol. 110 (2005) 529–554.
[5] D.P. Bentz, Influence of curing conditions on water loss and hydration in cement pastes with and without fly ash substitution NISTIR 6886, NIST, Gaithersburg, MD, 2002.
[6] W.C. Hansen, The chemistry of sulfate resisting Portland cements: in performance of concrete resistance of concrete to sulfate and other environmental conditions, in: E.G. Swenson (Ed.), A Symposium in Honour of Thorbergur Thorvaldson, University of Toronto Press, 1968, pp. 18–55.
[7] P.J.M. Monteiro, Scaling and saturation laws for the expansion of concrete exposed to sulfate attack, Proc. Natl. Acad. Sci. U.S.A. 103 (31) (2006) 11467–11472.
[8] M. Collepardi, A state-of-the-art review on delayed ettringite attack on concrete, Cem. Concr. Compos. 25 (2003) 401–440.
[9] M. Santhanam, M.D. Cohen, J. Olek, Effects of gypsum formation on the performance of cement mortars during external sulfate attack, Cem. Concr. Res. 33 (2003) 325–332.
[10] J. Skalny, J. Marchand, I. Older, Sulfate attack on concrete, in: Modern Concrete Technology Series, Spon Press, London, 2002.
[11] A.M. Neville, The confused world of sulfate attack on concrete, Cem. Concr. Res. 34 (2004) 1275–1296.
[12] ACI 201.2R-01, Guide to Durable Concrete, American Concrete Institute. Farmington Hills, MI.
[13] M.D. Cohen, B. Mather, Sulfate attack on concrete research needs, ACI Mater. J. 88 (1) (1991) 62–69.
[14] M. Pauri, M. Collepardi, Thermo-hygrometrical stability of thaumasite and ettringite, vol. 86, Il Cement, 1989, pp. 177–184.
[15] J.R. Clifton, J.M. Pommersheim, Sulfate attack of cementitious materials: volumetric relations and expansions NISTIR 5390, NIST, Gaithersburg, MD, 1994.
[16] K. Ramyar, G. Inan, Sodium sulfate attack on plain and blended cements, Build. Environ. 42 (2007) 1368–1372.
[17] J.G. Cabrera, C. Plowman, The mechanism and rate of attack of sodium sulfate solution on cement and cement/p FA pastes, Adv. Cem. Res. 1 (3) (1988) 171–179.
[18] T. Patzias, The development of ASTM method C1012 with recommended acceptance limits for sulfate resistance of hydraulic cement, Cem. Concr. Aggr. 13 (1) (1991) 50–57.

[19] Neural Network Toolbox User's Guide, Version 4 For use with MATLAB. Professor Martin Hagan of Oklahoma State University, Howard Demuth and Mark Beale, 1996, <www.mathworks.com>.
[20] W.S. McCulloch, W.H. Pitts, A logical calculus of the ideas immanent in nervous activity, Bulletin of Mathematical Biophysics 5 (1943) 115–133.
[21] I. Jung, G.N. Wang, Pattern classification of back-propagation algorithm using exclusive connecting network, Int. J. Comp. Sci. Eng. 2 (2) (2008) 76–80.
[22] A. Oztas, M. Pala, E. Özbay, E. Kanca, N. Çalar, M.A. Bhatti, Predicting the compressive strength and slump of high strength concrete using neural network, Constr. Build. Mater. 20 (2006) 769–775.
[23] S.C. Lee, Prediction of concrete strength using artificial neural networks, Eng. Struct. 25 (2003) 849–857.
[24] J. Kasperkiewics, J. Racz, A. Dubrawski, HPC strength prediction using ANN, ASCE J. Comp. Civil Eng. 9 (4) (1995) 279–284.
[25] S. Lai, M. Serra, Concrete strength prediction by means of neural network, Constr. Build. Mater. 11 (2) (1997) 93–98.
[26] I.C. Yeh, Modeling concrete strength with augment neuron networks, J. Mater. Civil Eng. 10 (4) (1998) 263–268.
[27] W.P.S. Dias, S.P. Pooliyadda, Neural networks for predicting properties of concretes with admixtures, Constr. Build. Mater. 15 (2001) 371–379.
[28] A. Baykasoglu, T. Dereli, S. Tanı, Prediction of cement strength using soft computing techniques, Cem. Concr. Res. 34 (2004) 2083–2090.
[29] Pala M, Özbay E, Özta_ A, Ishak YM. Appraisal of long-term effects of fly ash and silica fume on compressive strength of concrete by neural networks. Constr. Build. Mater. (2009), http://dx.doi.org/10.1016/j.conbuildmat.08.009.